Short Research Report

A model of longitudinal hemodynamic alterations after mild traumatic brain injury in adolescents

Journal of Concussion
Volume 3: 1–7

DOI: 10.1177/2059700219838654
journals.sagepub.com/home/ccn
SAGE

Corey M Thibeault, Samuel Thorpe, Nicolas Canac, Michael J O'Brien, Mina Ranjbaran, Seth J Wilk and Robert B Hamilton

Abstract

There is an unquestionable need for quantitative biomarkers of mild traumatic brain injuries. Something that is particularly true for adolescents – where the recovery from these injuries is still poorly understood. However, within this population, it is clear that the vasculature is distinctly affected by a mild traumatic brain injury. In addition, our group recently demonstrated how that effect appears to show a progression of alterations similar but in contrast to that found in severe traumatic injuries. Through measuring an adolescent population with transcranial Doppler ultrasound during a hypercapnia challenge, multiple phases of hemodynamic dysfunction were suggested. Here, we create a generalized model of the hemodynamic responses by fitting a set of inverse models to the dominant features from that work. The resulting model helps define the multiple phases of hemodynamic recovery after a mild traumatic brain injury. This can eventually be generalized, potentially providing a diagnostic tool for clinicians tracking patient's recovery, and ultimately, resulting in more informed decisions and better outcomes.

Keywords

Traumatic brain injury, vascular reactivity, cerebral blood flow autoregulation, blood flow, cerebral blood flow velocity

Date received: 10 May 2018; accepted: 19 February 2019

Introduction

The complexities of traumatic brain injuries (TBI) impede not only their diagnosis but their treatment as well. Adding to this is the relatively coarse classifications of severe, moderate, and mild that belie the heterogeneity of these injuries. However, one commonality between these classes is that the neurovasculature is affected in each.[1–13] Unfortunately, the similarity ends there. Recent results from our group[14] and others,[12,15–17] have suggested that in the mild or concussive classification (mTBI), the vascular and hemodynamic alterations contrast those found in moderate and severe cases. An understanding of that disparity as well as a better depiction of the vascular recovery after an mTBI is essential for developing diagnostic and prognostic biomarkers.

Current methods of diagnosing an mTBI rely on functional biomarkers (i.e. symptom reporting and neurocognitive testing). However, it is now apparent that a physiological dysfunction leaving patients vulnerable to successive injuries may still exist in the absence of measurable symptoms.[18] In particular, it has been found that cerebral blood flow (CBF) alterations can remain after clinical symptoms have subsided.[19–21] But before a comprehensive biomarker based on vascular dysfunction can be utilized, a more complete understanding of the underlying pathophysiology is needed. In this work, we are presenting a hypothesis of the hemodynamic progression adolescents undergo after suffering a concussion as measured by transcranial Doppler (TCD) ultrasound. To facilitate this, we

Neural Analytics, Inc., Los Angeles, USA

Corresponding author:
Corey M Thibeault, Neural Analytics, Inc., 2440 S Sepulveda Blvd, Suite 115, Los Angeles, CA 90064, USA.
Email: Corey@neuralanalytics.com

fit inverse models to the significant features extracted from a previous population level study.[14] The resulting series of models provides a generalized system for describing how TCD can capture the different phases of hemodynamic dysfunction after a concussion. The intention is that this model will not only result in testable hypotheses but also the start of a diagnostic aid for clinicians to evaluate patient recovery.

Materials and methods

Participants

Subjects between the ages of 14 and 19 years old were recruited from clinics and high schools in the Los Angeles, California area. The cases consisted of clinically diagnosed mTBI evaluated by independent physicians. There were a total of 70 subjects in this group (64% male), with some scanned multiple times over the course of their recovery. This resulted in a total of 187 scans, with a median of two scans per subject, spanning 1 h to 30 days after the injury. The control group was composed of 109 age matched subjects (89% male), who had no history of a head injury in the preceding 12 months. Data collection and processing were approved by Western Institutional Review Board (IRB #20141111).

Data collection

TCD data were collected with 2 MHz ultrasound probes held in place by an adjustable headband. The middle cerebral arteries were insonated transtemporally by ultrasound technicians. A breath-holding protocol was initiated after a 5-min baseline period of normal breathing. To ensure compliance with the breath-holding, end-tidal CO_2 was collected through a nasal cannula using a Nonin RespSense Capnometer. The data streams and clinical measures were collected with a custom codebase running on the Windows operating system.

Protocol

The breath-holding protocol was comprised of the sections illustrated in Figure 1. This started with a 5-min baseline section where subjects were instructed to breathe normally through their nose. Normal inspiration can help limit the Valsalva effect which would cause an initial decrease in CBF and lead to an underestimation of reactivity.[22] During the breath-holding portion of the protocol, subjects were instructed to take a normal breath and hold it for 25 s, followed by a 35-s period of normal breathing. This was repeated four times.

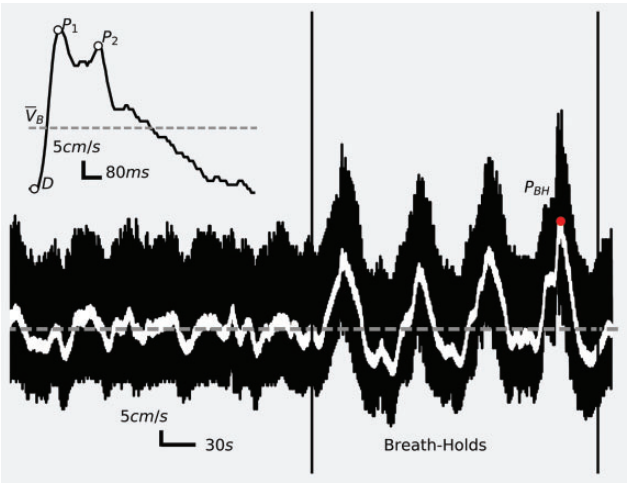

Figure 1. Experimental protocol and representative response. Example of measured CBFV values during an experiment for a single subject, solid black trace. The initial baseline period is followed by four breath-hold challenges indicated by the two solid vertical black lines. The low-pass filtered signal used for *BHI* calculations is overlaid by the solid white line. With the baseline mean velocity indicated by the dashed gray line. The peak used for CVR calculations is marked by the red circle labeled P_{BH}. Beat level features (inlay): The pulsatile analysis is completed on the baseline beats. The example beat, solid black trace, illustrates the systolic peak (P_1), the diastolic valley (D), and second peak (P_2). The beat mean velocity is indicated by the dashed gray line labeled $\bar{V}_B$.

Analysis

The analysis of the baseline section of the examinations began with the identification of individual beats – completed with a software package developed in Python. The two features explored in this work were the Gosling Pulsatility Index (*PI*) and the P2 Ratio (*P2R*). These are computed using the pulse features illustrated in Figure 1.

PI is a complex metric that is modulated by a combination of cerebral perfusion pressure, cerebrovascular resistance, arterial bed compliance, heart rate, and the pulse amplitude.[23] It is calculated by

$$PI = (P_1 - D)/\bar{V} \quad (1)$$

where P_1 is the systolic peak, D is the diastolic valley, and $\bar{V}$ is the mean velocity of the pulse. $P2R$ is a metric that relates the second observed waveform peak, P_2, with the systolic peak referred to here as P_1. It is possibly related to distal bed compliance but currently there is no clear physiological link to changes in $P2R$. It is computed using

$$P2R = P_2/P_1 \quad (2)$$

To evaluate the cerebrovascular reactivity (CVR), the Breath-Hold Index (*BHI*) is computed by first

extracting the highest peak, P_{BH}, between the four breath-hold regions from the low-pass filtered cerebral blood flow velocity (CBFV); see Figure 1. The mean velocity over the entire baseline, $\bar{V}_{BL}$, is computed, and the *BHI* can then be found from

$$BHI = \frac{P_{BH} - \bar{V}_{BL}}{\bar{V}_{BL}} \quad (3)$$

Statistical analysis of the population data was completed using the Scipy library.[24] Cases and controls were compared using the Wilcoxon–Mann–Whitney two-sample rank-sum test. Model fitting was completed by the Levenberg–Marquardt nonlinear least squares minimization method using the lmfit library.[25] The different candidate inverse models were compared using the Bayesian information criterion (BIC).[26] In this case, the models were selected from different classes of functions and compared using the BIC. This inherently penalizes free parameters but a specific emphasis was placed on reducing the opportunity for over-fitting when selecting the functions to be considered. The goal was to select inverse models that offered the best opportunity for generalization when applied to individual subjects in the future. As models were explored, free parameters were added and compared with previous models using the BIC. If the change was small, the model was discarded in favor of the simpler option. Confidence intervals were computed for the model fit for 95% confidence using the method described by Wolberg[27] implemented in the lmfit library.

Results

Population results

The population results were previously published in Thibeault et al.,[14] but are reported here for completeness. There was no significant difference in age between the two groups (controls: 16 years, mTBI: 16.21 years, $U = 0.18$, $P = 0.86$). As the extracted features are grouped by days post-injury, two phases of injury progression appear. The first is captured within the initial 48 h where both the *PI* ($P < 0.01$) and *P2R* ($P < 0.01$) values are significantly different than the controls, (Figure 2(a) and (b)). In addition, during this period *PI* and the *P2R* were uncorrelated based on Pearson's correlation analysis ($rp = -0.36$; $P = 0.23$). After 48 h these are no longer distinguishable from the healthy controls.

This delineates the second phase of recovery that is captured by the *BHI*, see Figure 2(c). During the period immediately following injury, the *BHI* is no different

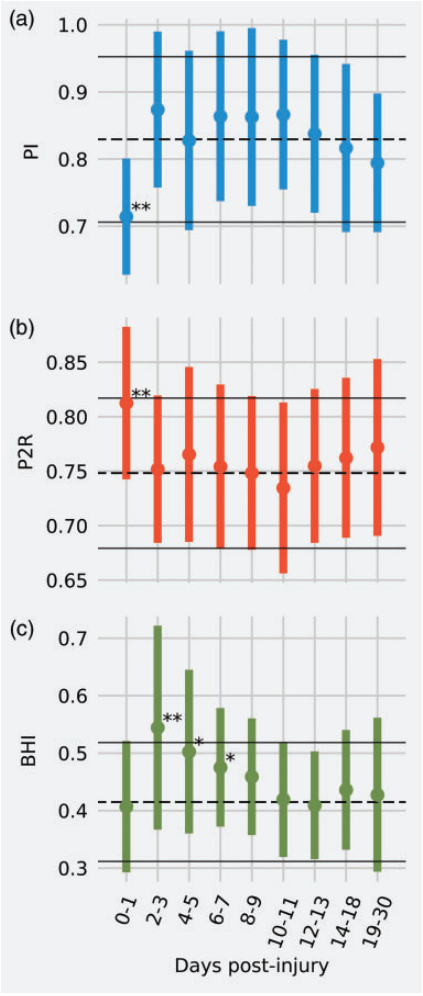

Figure 2. Population results: (a) *PI*, (b) *P2R*, and (c) *BHI*. **$P < 0.01$, *$P < 0.05$. The dashed black lines represent the control population mean with interquartile range marked by the surrounding solid black lines.

than the controls ($P = 0.67$). However, two days after injury there is an increase in *BHI* that is significantly different than the controls ($P < 0.01$). This increase decayed over days 4–5 ($P = 0.014$) and days 6–7 ($P = 0.018$). Finally, at days 8–9 the injured population is no longer statistically differentiable from the controls.

Feature model development

Using these three features from the population results above, a set of models was developed to describe, in general, how these variables change over the course of recovery. For *PI*, a model of the form

$$PI = a + \frac{b}{b + e^{-\alpha t}} \quad (4)$$

was fit to the population data. Here, t is the time in days and a, b, and α are the model coefficients fit by the

Levenberg–Marquardt minimization. Figure 3(a) presents the model curve with the 95% confidence intervals. For this model the best fit parameters were $a = -0.158$, $b = 5.784$, and $\alpha = 0.997$. Similarly, *P2R* was found using an inverted form of the *PI* model

$$P2R = -a - \frac{b}{b + e^{-\alpha t}} \tag{5}$$

The variables have the same definitions as in equation (4) and the results of the model fit are illustrated in Figure 3(b). The best fit resulted in the values $a = -1.769$, $b = 16.946$, and $\alpha = 0.288$. Finally, the *BHI* was fit with a model of the form

$$BHI = a + bte^{-\alpha t} \tag{6}$$

where, t, a, b, and α are the same as in equations (4) and (5). Figure 3(c) illustrates the resulting model and the best fit variables are $a = 0.42$, $b = 0.13$, and $\alpha = 0.45$.

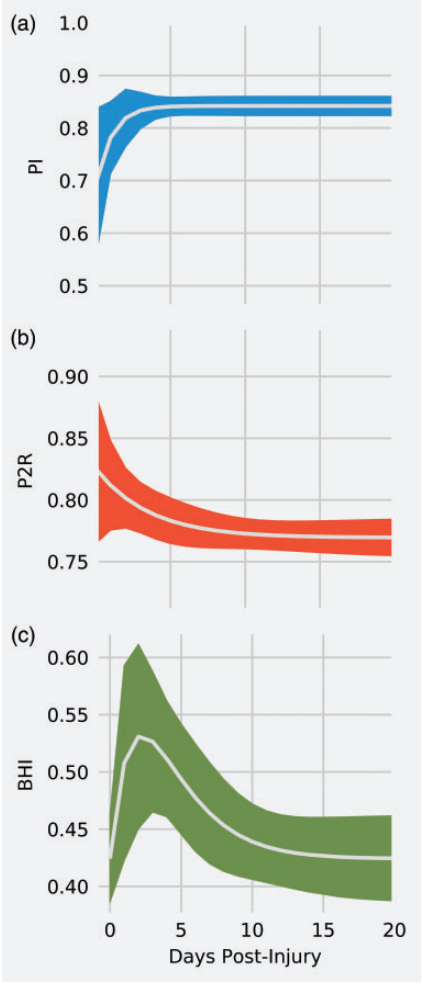

Figure 3. Model fits: (a) *PI*, (b) *P2R*, and (c) *BHI*. Solid white lines are the best fit lines. The ribbons are the 95% confidence intervals for the best fit model.

Recovery model

Using the results above, we are proposing that there are three phases of hemodynamic alterations captured with TCD after an mTBI that can be described by these models. Plotting the feature models in terms of percent change from controls reveals this generalized progression of hemodynamic recovery; see Figure 4. This overall model is suggesting that in the stereotypical case, subjects will go through two phases before reaching hemodynamic stability in phase III. In the other cases, we are hypothesizing that this third phase will mark a transition into a chronic period of dysfunction not observed in this dataset.

Phase I. The immediate symptoms of a concussion are generally attributed to microstructural changes in the neural tissue.[13] During the initial phase of hemodynamic dysfunction, we are hypothesizing that that mechanical insult noticeably affects the distal vasculature. These proposed alterations to the arterioles are captured by either *PI*, *P2R*, or both. *PI* has historically been associated with cerebrovascular resistance[28,29] as well as the remote vasculature.[23] Similarly, *P2R* has been theorized to be associated with the compliance of those resistance vessels.[30] These are both areas that could be affected by a sufficient biomechanical force. This is the first time this phase of dysfunction has been proposed in mTBI.

In the population measured here, *PI* had a higher percent change of controls than *P2R*. This suggests that *PI* has more predictive utility. Our previous work demonstrated that these features were also

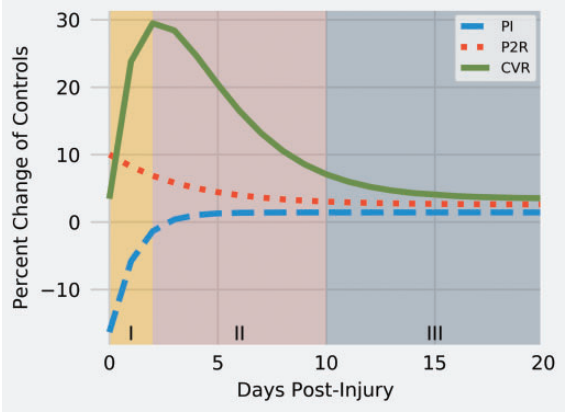

Figure 4. Model of hemodynamic recovery after concussive injury. The models are represented in percent change from controls. The separation of the three hemodynamic phases of recovery is illustrated by the blocks with corresponding labels along the x-axis.

uncorrelated during this period.[14] Something we hypothesized may be indicative of different aspects, or types of injuries, being captured by TCD. How this manifests into a stronger change in *PI* is unclear but is something that is being explored further in future studies.

Phase II. The transition to phase II in this model is identified by an increase in reactivity and a return of *PI* and *P2R* to basal levels. Previously we have hypothesized that this was related to the neurometabolic cascade that occurs after a TBI. There are a number of metabolic responses to a head injury, and in severe injuries there is a disruption of the nitric oxide signaling pathway of the vasculature. However, in those cases the smooth muscle cells still respond to nitric oxide but endothelial cells do not produce enough nitric oxide synthase (NOS). Ultimately, resulting in a reduction of CVR. It is tempting to suggest an analogous, although opposite, dysfunction in the NOS pathway for mTBI. An increase in NOS in the endothelium was proposed by Militana et al.[12] and would result in an increase in reactivity. However, the process resulting in this increase is not clear. This is something that will be explored in future studies.

Phase III. The transition to phase III is marked by a return to normal CVR. In this instance, the model is reaching a basal level similar to the onset of the injury. However, it is more likely that subjects do not return to the same level of reactivity as pre-injury. This will be explored further in future studies. For this population, the mTBI subjects were no longer differentiable after day 7 but, in general, mTBI patients appear to recover within 7–14 days after injury.[18,31] The shorter time scale observed here is likely a byproduct of the relatively mild injuries suffered by the population. Of the 70 mTBI subjects only six reported loss of consciousness in the 12 months preceding the scan. Of those, one subject reported having to be hospitalized, four lost consciousness for less than 1 min, and one subject chose to not provide a response. As this model is refined, or applied to individuals as part of recovery tracking, the heterogeneity of the injuries will be captured. We hypothesize that regardless of the time course of recovery, concussive injuries will result in these hemodynamic phase transitions.

This model fails to elucidate how chronic subjects transition into phase III. Studies have shown that patients suffering from chronic symptoms have lowered CVR.[16] Additionally, this has been found using TCD in the study by Bailey et al.[10] The third phase of hemodynamic recovery presented by this model represents an eventual plateau to a healthy basal CVR. For chronic subjects, this would be a transition into a hyporeactive phase. The time course of that transition is unclear; however, future studies will include a chronic population to help fill in the recovery model.

Discussion

The most surprising and novel aspect of this model is the initial period of dysfunction and how it differs from other studies of hemodynamics in mTBI. The hyperacute dataset provides a unique insight into the progression of the CBFV response that has not been demonstrated before. Combined with the acute, and subacute scans, a progression of hemodynamics after concussion emerges.

Although the dysfunction described in phase I has only been demonstrated in our previous work,[14] other studies of hemodynamics have recently revealed similar increases in CVR (as shown in phase II of the recovery model). In a pilot study of seven subjects using magnetic resonance imaging (MRI), Militana et al.[12] also found hyperreactivity. Similarly, the small CVR study utilizing MRI from Mutch et al.[16] showed that two of the acute stage subjects with relatively severe injuries, measured at days 7 and 13 post-injury, had an increase in CVR. However, in a subsequent study that group found increased CVR for multiple concussed adolescents using MRI.[17] In each of these studies, time since injury was not considered, only that the subjects were still symptomatic.

There have also been a number of studies that have found differences in concussed subjects utilizing TCD. Len et al. found alterations in CVR under both hypocapnia[11] and hypercapnia.[15] Similarly, Bailey et al.[10] showed lowered CVR in a population suffering from chronic mTBI.

An aspect that this model fails to take into account is the differences in individuals or the heterogeneity of their injuries. The broad classification of mTBI encompasses a variety of injuries that likely affect the vasculature differently. These differences include both the amplitude of the dysfunction and the time course of recovery. Although we hypothesize that these phases of recovery are generalizable, the coefficients of the population models are likely not. It appears, however, that this model of hemodynamic recovery can accurately predict the injury progression. A follow-up study is exploring how well these models fit subjects with high-density longitudinal data. Additionally, the age of the population driving this model is a limiting factor. The dependence on age in CBF regulation has been demonstrated and in general clinicians need to be aware of those when managing pediatric patients.[32,33] It is not clear if the responses found in this model are applicable to other populations.

There is a clear need for biomarkers of dysfunction after concussive injuries to aid clinicians.[34] The results of this study illustrate the potential for TCD in collecting actionable information that could be the foundation for diagnostic and prognostic biomarkers. Clinically, the models presented here may one day help healthcare professionals treating adolescents interpret the different phases of dysfunction. With a better understanding of the progress patients are making, more informed decisions on treatments, as well as return to activity timing, can be made. As a monitoring tool, the free parameters of these models could be fit to an individual's recovery data to continuously observe progress. This would add a quantitative measure of vascular function and expected recovery to complement the current standard of care. In addition, this method could help identify patients who deviate from that expected model who may require additional intervention.

Acknowledgements

We would like to thank Mateo Scheidt, Leonardo Martinez, Danielle Seth-Hunter, Amanda Wu, and Aaron Green for assisting with data collection in this study. Additionally, we would like to thank Dan Hanchey, Shankar Radhakrishnan, Ben Delay, Sirian Wang, and Svetlana Akim for their software and technical assistance. The NIH had no role in the design and conduct of the study; collection, management, analysis, and interpretation of the data; preparation, review, or approval of the manuscript; and decision to submit the manuscript for publication. The content is solely the responsibility of the authors and does not necessarily represent the official views of the National Institutes of Health.

Authors' contributions

CMT had full access to all the data in the study and takes responsibility for the integrity of the data and the accuracy of the data analysis. Study concept and design: RBH. Analysis: CMT. Interpretation of data: CMT, RBH. Drafting of the manuscript: CMT. Critical revision of the manuscript for important intellectual content: RBH, SJW. Statistical analysis: CMT. Technical or material support: ST, MJO'B, NC, MR, SJW. Study supervision: RBH, CMT.

Declaration of conflicting interests

The author(s) declared the following potential conflicts of interest with respect to the research, authorship, and/or publication of this article: At the time that this research was conducted, Corey M Thibeault, Samuel Thorpe, Michael J O'Brien, Nicolas Canac, Mina Ranjbaran, Seth J Wilk, and Robert B Hamilton were employees of, and either hold stock or stock options in, Neural Analytics, Inc.

Funding

The author(s) disclosed receipt of the following financial support for the research, authorship, and/or publication of this article: This work was supported by the National Institute of Neurological Disorders and Stroke of the National Institutes of Health under award numbers 1R43NS092209-01 and 2R44NS092209-02.

ORCID iD

Corey M Thibeault http://orcid.org/0000-0002-3916-901X

References

1. Meier TB, Bellgowan PSF, Singh R, et al. Recovery of cerebral blood flow following sports-related concussion. *JAMA Neurol* 2015; 72: 530–538.
2. Wang Y, Nelson LD, LaRoche AA, et al. Cerebral blood flow alterations in acute sport-related concussion. *J Neurotrauma* 2016; 33: 1227–1236.
3. Barkhoudarian G, Hovda DA and Giza CC. The molecular pathophysiology of concussive brain injury – an update. *Phys Med Rehabil Clin N Am* 2016; 27: 373–393.
4. Maugans TA, Farley C, Altaye M, et al. Pediatric sports-related concussion produces cerebral blood flow alterations. *Pediatrics* 2011; 129: 28–37.
5. Zaaroor M, Mahamid E, Shik V, et al. Course of cerebral blood flow and metabolism following severe brain injury. Correlation with neurological function and outcome. *Indian J Neurotrauma* 2007; 4: 25–29.
6. Kenney K, Amyot F, Haber M, et al. Cerebral vascular injury in traumatic brain injury. *Exp Neurol* 2016; 275: 353–366.
7. Werner C and Engelhard K. Pathophysiology of traumatic brain injury. *Br J Anaesth* 2007; 99: 4–9.
8. Martin NA, Patwardhan RV, Alexander MJ, et al. Characterization of cerebral hemodynamic phases following severe head trauma: hypoperfusion, hyperemia, and vasospasm. *J Neurosurg* 1997; 87: 9–19.
9. Lee JH, Kelly DF, Oertel M, et al. Carbon dioxide reactivity, pressure autoregulation, and metabolic suppression reactivity after head injury: a transcranial Doppler study. *J Neurosurg* 2001; 95: 222–232.
10. Bailey DM, Jones DW, Sinnott A, et al. Impaired cerebral haemodynamic function associated with chronic traumatic brain injury in professional boxers. *Clin Sci* 2013; 124: 177–189.
11. Len TK, Patrick Neary J, Asmundson GJG, et al. Cerebrovascular reactivity impairment after sport-induced concussion. *Med Sci Sports Exercise* 2011; 43: 2241–2248.
12. Militana AR, Donahue MJ, Sills AK, et al. Alterations in default-mode network connectivity may be influenced by cerebrovascular changes within 1 week of sports related concussion in college varsity athletes: a pilot study. *Brain Imaging Behav* 2016; 10: 559–568.
13. Giza CC and Hovda DA. The new neurometabolic cascade of concussion. *Neurosurgery* 2014; 75: S24–S33.
14. Thibeault CM, Thorpe S, O'Brien MJ, et al. A cross-sectional study on cerebral hemodynamics after mild

traumatic brain injury in a pediatric population. *Front Neurol* 2018; 9: 200.
15. Len TK, Neary JP, Asmundson GJG, et al. Serial monitoring of CO2 reactivity following sport concussion using hypocapnia and hypercapnia. *Brain Inj* 2013; 27: 346–353.
16. Mutch WAC, Ellis MJ, Ryner LN, et al. Longitudinal brain magnetic resonance imaging CO2 stress testing in individual adolescent sports-related concussion patients: a pilot study. *Front Neurol* 2016; 7: 107.
17. Mutch WAC, Ellis MJ, Ryner LN, et al. Patient-specific alterations in CO2 cerebrovascular responsiveness in acute and sub-acute sports-related concussion. *Front Neurol* 2018; 9: 23.
18. McCrea M, Prichep L, Powell MR, et al. Acute effects and recovery after sport-related concussion: a neurocognitive and quantitative brain electrical activity study. *J Head Trauma Rehabil* 2010; 25: 283–292.
19. DeWitt DS and Prough DS. Traumatic cerebral vascular injury: the effects of concussive brain injury on the cerebral vasculature. *J Neurotrauma* 2003; 20: 795–825.
20. Markus HS and Harrison MJ. Estimation of cerebrovascular reactivity using transcranial Doppler, including the use of breath-holding as the vasodilatory stimulus. *Stroke* 1992; 23: 668–673.
21. Kraus MF, Susmaras T, Caughlin BP, et al. White matter integrity and cognition in chronic traumatic brain injury: a diffusion tensor imaging study. *Brain* 2007; 130: 2508–2519.
22. Settakis G, Lengyel A, Molnár C, et al. Transcranial Doppler study of the cerebral hemodynamic changes during breath-holding and hyperventilation tests. *J Neuroimaging* 2002; 12: 252–258.
23. de Riva N, Budohoski KP, Smielewski P, et al. Transcranial Doppler pulsatility index: What it is and What it isn't. *Neurocritical Care* 2012; 17: 58–66.
24. Oliphant TE. Python for scientific computing. *Comput Sci Eng* 2007; 9: 10–20.
25. Newville M, Stensitzki T, Allen DB, et al. LMFIT: non-linear least-square minimization and curve-fitting for Python. *Astrophysics Source Code Library*, 2016.
26. Schwarz G. Estimating the dimension of a model. *Ann Statist* 1978; 6: 461–464.
27. Wolberg J. *Data analysis using the method of least squares: extracting the most information from experiments*. Berlin: Springer Science & Business Media, 2006.
28. Giller CA, Hodges K and Batjer HH. Transcranial Doppler pulsatility in vasodilation and stenosis. *J Neurosurg* 1990; 72: 901–906.
29. Lim M-H, Cho YI and Jeong S-K. Homocysteine and pulsatility index of cerebral arteries. *Stroke* 2009; 40: 3216–3220.
30. Hamilton R, Baldwin K, Fuller J, et al. Intracranial pressure pulse waveform correlates with aqueductal cerebrospinal fluid stroke volume. *J Appl Physiol* 2012; 113: 1560–1566.
31. Belanger HG and Vanderploeg RD. The neuropsychological impact of sports-related concussion: a meta-analysis. *J Int Neuropsychol Soc* 2005; 11: 345–357.
32. Mandera M, Larysz D and Wojtacha M. Changes in cerebral hemodynamics assessed by transcranial Doppler ultrasonography in children after head injury. *Child's Nerv Syst* 2002; 18: 124–128.
33. Manzanero S, Elkington LJ, Praet SF, et al. Post-concussion recovery in children and adolescents: a narrative review. *J Concussion* 2017; 1: 205970021772687.
34. McCrory P, Meeuwisse W, Dvořák J, et al. Consensus statement on concussion in sport – the 5 international conference on concussion in sport held in Berlin, October 2016. *Br J Sports Med* 2017; 51: 838–847.